5,12-Dihydroindolo[3,2-a]carbazole : A promising scaffold for the design of visible light photoinitiators of polymerization

Fatima Hammoud, Akram Hijazi, Sylvain Duval, Jacques Lalevée, Frédéric Dumur

5,12-Dihydroindolo[3,2-a]carbazole : A promising scaffold for the design of visible light photoinitiators of polymerization

Fatima Hammoud [1,2,3], Akram Hijazi [3], Sylvain Duval [4], Jacques Lalevée [1,2]* and Frédéric Dumur [5]*

[1] Université de Haute-Alsace, CNRS, IS2M UMR 7361, F-68100 Mulhouse, France
[2] Université de Strasbourg, France
[3] EDST, Université Libanaise, Campus Hariri, Hadath, Beyrouth, Liban
[4] Université de Lille, CNRS, Centrale Lille, ENSCL, Univ. Artois, UMR 8181 - UCCS - Unité de Catalyse et Chimie du Solide, F-59000 Lille, France
[5] Aix Marseille Univ, CNRS, ICR UMR7273, F-13397 Marseille France

* Correspondence: Jacques.lalevee@uha.fr, frederic.dumur@univ-amu.fr

Abstract

5,12-Dihydroindolo[3,2-*a*]carbazole is a polycyclic structure combining in its scaffold two carbazole moieties sharing a fused aromatic ring. Since the pioneering works reported in 2019 on this structure concerning the substitution of the two carbazoles by similar functional groups, no recent investigation has been devoted to asymmetrize the substitution of the two carbazoles. In this work, a series of 13 compounds based on the 5,12-dihydroindolo[3,2-*a*]carbazole scaffold is presented. By carefully controlling the reaction conditions, functional groups such as a formyl, a nitro or an acetyl group could be selectively introduced on one of the two carbazoles. By combining X-ray diffraction and 2D NMR experiments, the higher reactivity of one of the two carbazoles could be clearly evidenced, enabling to generate asymmetrically substituted structures. Thanks to this unprecedented approach on the 5,12-dihydroindolo[3,2-*a*]carbazole scaffold, the absorption of the resulting dyes could be shifted towards the visible range whereas the parent structure (5,12-dihexyl-6,7-diphenyl-5,12-dihydroindolo[3,2-*a*]carbazole) exhibits a strongly UV-centered absorption. In light of their visible light absorption properties, several dyes have been examined as photoinitiators of polymerization activable at 405 nm and under low light intensity in two-component photoinitiating systems for the free radical polymerization of acrylates or the cationic polymerization of epoxides. Chemical mechanisms supporting the different polymerization processes have been fully elucidated by combining several techniques including cyclic

voltammetry, UV-visible absorption and photoluminescence spectroscopy as well as photolysis experiments.

Keywords

Carbazole, photopolymerization, dyes, asymmetric substitution

1. Introduction

During the last decades, carbazole which is a tricyclic aromatic heterocyclic compound comprising two aromatic rings fused on either side of a five-membered ring bearing a nitrogen as a ring hetero atom has the focus of intense research efforts.[1] Interest for carbazole is notably supported by the different applications in which this polyaromatic structure is involved including Organic Electronics (Organic Light-Emitting Diodes (OLEDs),[2–7] Organic Photovoltaics (OPVs),[8–10] Organic Field Effect Transistors (OFETs)),[11–13] Non Linear Optics[14–17] to compounds exhibiting biological activities (antimicrobial, antiepileptic, anti-inflammatory, antihistaminic, antidiarrheal, antitumor, analgesic and neuroprotective properties),[18] solid state emitters for two-photon imaging[19] and photoinitiators of polymerization.[20] From a photophysical viewpoint, carbazole is characterized by a wide bandgap[21] and a high triplet energy level[22,23] which has been advantageously used for the design of hosts materials for triplet emitters for OLEDs, enabling to prevent back energy transfer from the triplet emitters to the host.[24] Carbazole is also extensively used for the design of polymeric hosts for OLEDs and, in this field, the most representative polymer is undoubtedly poly(*N*-vinylcarbazole) (PVK)[25] which exhibits a good film-forming ability, a high morphological stability and a high thermal decomposition temperature.[26] When used as photoinitiators of polymerization, carbazole was notably used as an electron donor for the design of push-pull dyes,[27–32] as a π-conjugated spacer to connect pyrenes or triphenylamines[33], enabling to generate polyaromatic structures of extended π-conjugation,[31] but also as a basis for the design of helicenes[34] or benzophenone derivatives.[35] Beyond the absorption property which is one of the key parameter governing the polymerization efficiency, migratability of photoinitiators within the polymer is another major issue that can adversely affect the potential use of polymers, especially for applications such as food packaging[36–38] or different biological applications[39]. In fact, photopolymerization constitutes an efficient and environmentally friendly approach to prepare polymers for food packaging. However, photoinitiators are often small molecules that can migrate in the foodstuff, even if not necessarily harmful. This migration is undesirable and the

subject of various legislative requirements. To address these issues, the development of macrophotoinitiators constitutes an efficient strategy. Indeed, the bigger the photoinitiator is, the more difficult the migration of photoinitiators within the polymer network is. In order to meet these requirements, oligomeric photoinitiators have notably been proposed.[40,41] Another efficient strategy consists in introducing crosslinkable functional groups onto photoinitiators.

However, if this strategy is appealing to reduce the migratability of small molecules, it also requires the photoinitiators to be chemically modified, what can constitute a challenge for certain photoinitiators.[42–48] When the synthesis of macrophotoinitiators is privileged as the option, in order to maximize the photoinitiating ability of macrophotoinitiators while minimizing the non-photoinitiating portion of the molecules, the combination of well-known photoinitiators within a unique molecule constitutes an efficient strategy. In this field, a relevant example has been proposed with truxene, which has notably been substituted with acridine-1,8-diones,[49] DMPA (2,2′-dimethoxy-2-phenyl acetophenone)[50] or pyrene.[51] By electronic coupling of the molecular orbitals of the truxene central core with that of the peripheral groups, a major enhancement of the molar extinction coefficients could be obtained, enabling to reduce the photoinitiator content. With aim at developing macromolecular photoinitiators based on carbazole, 5,12-dihydroindolo[3,2-a]carbazole which comprises two carbazole units sharing a fused aromatic ring is a perfect candidate. This structure, reported for the first time in 2019,[52] has notably been studied for its regioselective *bis*(acetylation) and *bis*(formylation) at the C2,9-positions. To date, no asymmetrically substituted derivatives of this structure (5,12-dihydroindolo[3,2-a]carbazole) have been reported yet. It has to be noticed that asymmetrically substituted carbazoles have already been reported in the literature as visible light photoinitiators of polymerization, but not on *bis*-carbazole structures. Thus, push-pull dyes based on carbazole have been reported as soon as 2013. [53] Final monomer conversions of 55% and 45% could respectively be obtained during the cationic polymerization of (3,4-epoxycyclohexane)methyl 3,4-epoxycyclohexylcarboxylate (EPOX) and the free radical polymerization of trimethylolpropane triacrylate (TMPTA) upon irradiation at 473 nm of photocurable resins comprising three-component carbazole/NVK/Ph_2I^+ photoinitiating systems (where NVK and Ph_2I^+ stand for *N*-vinylcarbazole and diphenyliodonium hexafluorophosphate).[54] While using indane-1,3-dione-based push-pull dyes, a TMPTA conversion of 58% could be obtained using three-component carbazole/NVK/Ph_2I^+ photoinitiating systems upon irradiation at 457 nm. Nitration of carbazole constitutes an efficient strategy to red-shift the absorption spectra of

carbazole and this strategy was notably reported with a series of four dyes in 2017.[32] Interestingly, the four carbazole derivatives could be used photoredox catalysts and comparison of the photoinitiating abilities of the four dyes with that of *bis*(2,4,6-trimethylbenzoyl)phenylphosphine oxide (BAPO) revealed the four dyes to outperform BAPO at 405 nm. Thus, by using two-component carbazole/(*t*-Bu)Ph_2I^+ photoinitiating systems (where (*t*-Bu)Ph_2I^+ stands for *bis*-(4-*tert*-butylphenyl)iodonium hexafluorophosphate, final monomer conversions ranging between 50 and 76% could be obtained during the cationic polymerization of EPOX, contrarily to 15% for BAPO in the same irradiation conditions. Asymmetrically substituted carbazoles exhibiting extended aromaticities were also examined in 2017 as photoinitiators activable at 405 nm for the cationic polymerization of EPOX .[29] In this series, an EPOX conversion of 57% could be obtained with a naphthalene-based dye while using two-component carbazole/(*t*-Bu)Ph_2I^+ photoinitiating systems. As interesting feature, colourless coatings could be obtained with this series of dyes, the carbazole derivatives being designed with weak electron-acceptors enabling to get high molar extinction coefficients at 405 nm while maintaining a low absorption beyond 420 nm. Similar performances were obtained for dyes based on 1,4-dimethyl-9*H*-carbazole.[30] In this case, best performances were obtained for a formyl-substituted carbazole and an EPOX conversion of 48% using two-component carbazole/(*t*-Bu)Ph_2I^+ photoinitiating systems at 405 nm. Once again, the formyl-substituted carbazole could outperform BAPO (15% conversion at 405 nm). While substituting carbazole with a BODIPY, polymerization reactions could be initiated with near-infrared lights, demonstrating the versatility of the carbazole scaffold for designing photoinitiating activable between 400 and 1100 nm.[55] In this work, a series of 5,12-dihydroindolo[3,2-*a*]carbazole derivatives asymmetrically substituted with different functional groups such as formyl, acetyl or nitro groups have been designed and synthesized. The different syntheses revealed the functionalization of the C2-position to be easier than the C9-position. By mean of this asymmetric substitution, dyes absorbing beyond 400 nm could be obtained. To evidence the interest of these new structures, photopolymerization experiments have been carried out upon irradiation at 405 nm.

2. Experimental part

2.1. Synthesis of the different dyes

For this study, 5,12-dihexyl-6,7-diphenyl-5,12-dihydroindolo[3,2-*a*]carbazole **C2** was selected as the parent structure. Notably, hexyl chains were selected to provide a sufficient solubility to this polyaromatic structure. It can be synthesized in one step, by alkylation of 6,7-

diphenyl-5,12-dihydroindolo[3,2-a]carbazole **C1** that was prepared in one step by an acid-catalyzed cycloaddition of two equivalents of indole with benzil, according to a procedure previously reported in the literature (See Scheme 1).[56] Interestingly, formylation of **C2** by mean of the Rieche method[57,58] that consists in treating **C2** with 1,1-dichloromethyl methyl ether in the presence of tin tetrachloride ($SnCl_4$) only furnished after one hour of reaction at -20°C 5,12-dihexyl-6,7-diphenyl-5,12-dihydroindolo[3,2-*a*]carbazole-2-carbaldehyde **C3** in moderate yield (35%), the rest corresponding to the unreacted starting compound **C2**. Conversely, by performing the reaction in the same conditions, but by stirring the solution at room temperature overnight, 5,12-dihexyl-6,7-diphenyl-5,12-dihydroindolo[3,2-*a*]carbazole-2,9-dicarbaldehyde **C4** could be selectively prepared in 67% yield.

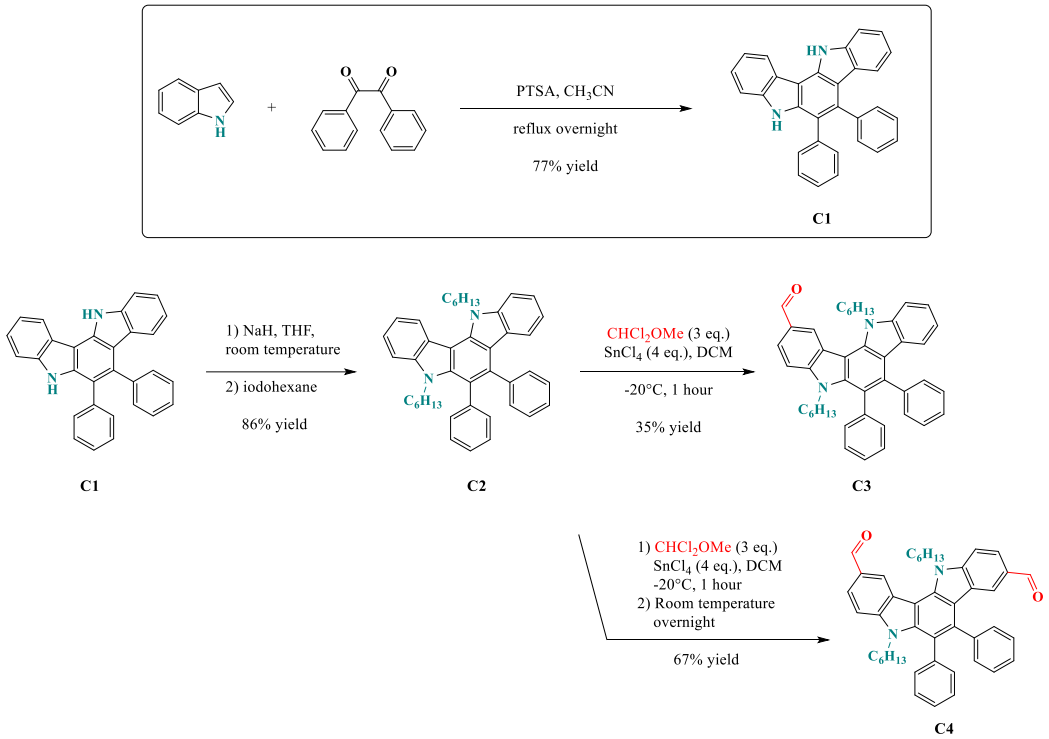

Scheme 1. Synthetic route to **C1-C4**.

In order to determine on which position (C2 or C9-positions) the formyl group was introduced on **C3**, 2D NMR experiments were carried out. As shown on the NOESY spectrum presented in the Figure 1, a NOESY peak could be clearly identified between the aromatic proton (proton 1) at 9.00 ppm adjacent to the formyl peak (10.19 ppm, proton 5) and the CH_2 group at 4.98 ppm (proton 4). It could thus be concluded that the formyl group was introduced at the C2-position. Indeed, if introduced at the C9 position, no through space interaction could occur with any of the CH_2 groups of the alkyl chains. By slow evaporation of chloroform,

crystals of **C3** could be obtained, confirming the previous assignment done by NMR spectroscopy (See Figure 2).

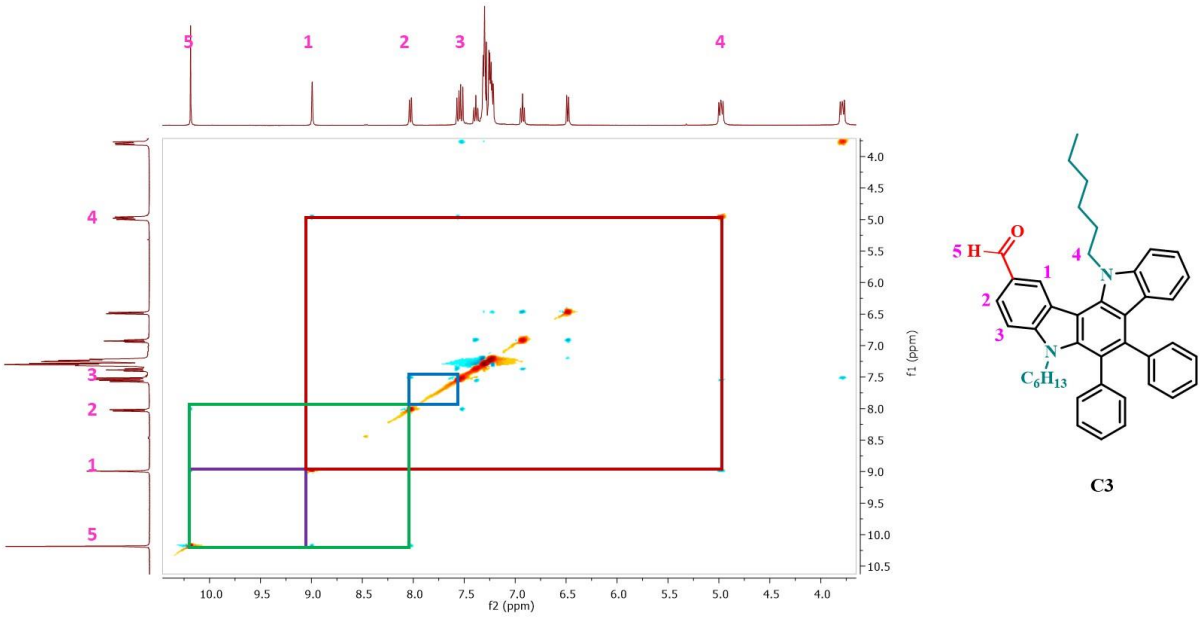

Figure 1. NOESY spectrum of **C3** recorded in $CDCl_3$ as the deuterated solvent.

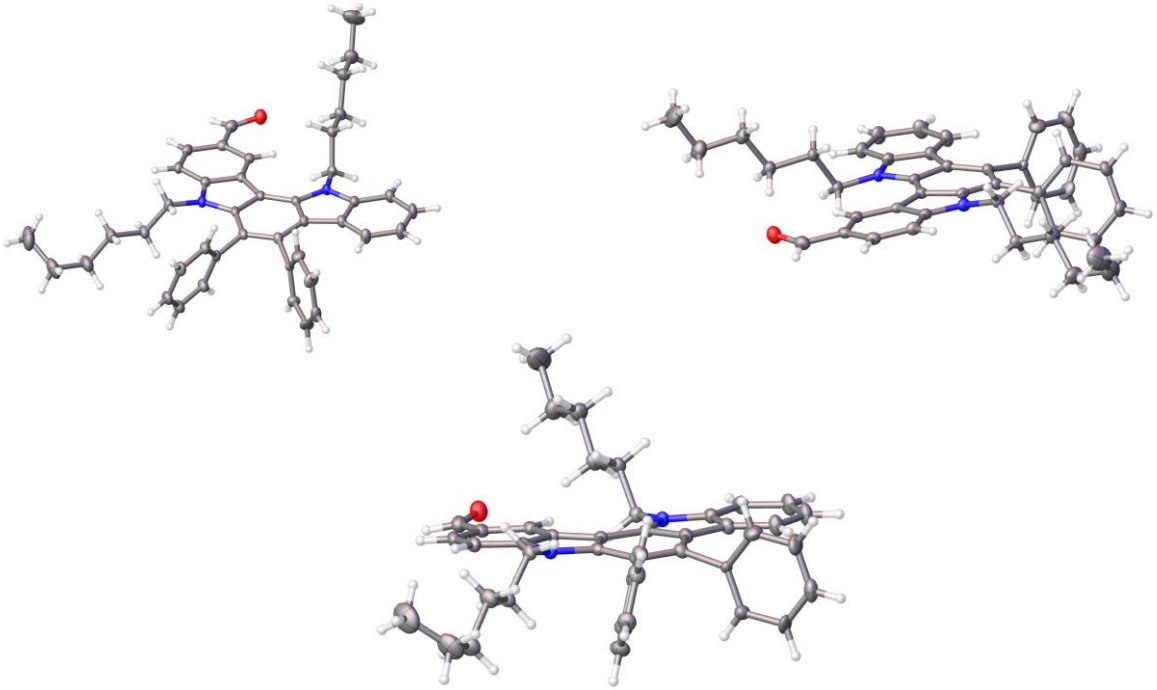

Figure 2. Crystal structure of **C3**.

Following these initial attempts, the possibility to selectively introduce other groups than a formyl group was examined. Notably, an acetyl group could be selectively introduced on **C5** in 42% yield while realizing a Friedel-Craft reaction with one equivalent of acetyl

chloride at room temperature overnight. However, formation of the second regioisomer **C5'** could also be evidenced. This isomer could only be obtained in 16% yield. As shown in the Figure 3, clear difference could be seen on their ^{1}H NMR spectra. Thus, if the acetyl group for the regioisomer at the C2-position could be detected at 2.78 ppm, conversely, a shift as high as 2.5 ppm could be demonstrated for the regioisomer at the C9-position, the acetyl group being detected at 2.19 ppm. Interestingly, comparison with the ^{1}H NMR spectrum of 1,1'-(5,12-dihexyl-6,7-diphenyl-5,12-dihydroindolo[3,2-*a*]carbazole-2,9-diyl)*bis*(ethan-1-one) **C5''** revealed the positions of the acetyl groups to be at similar positions to that of the *bis*-substituted compound **C5''**. Thus, acetyl groups are respectively detected at 2.77 and 2.20 ppm.

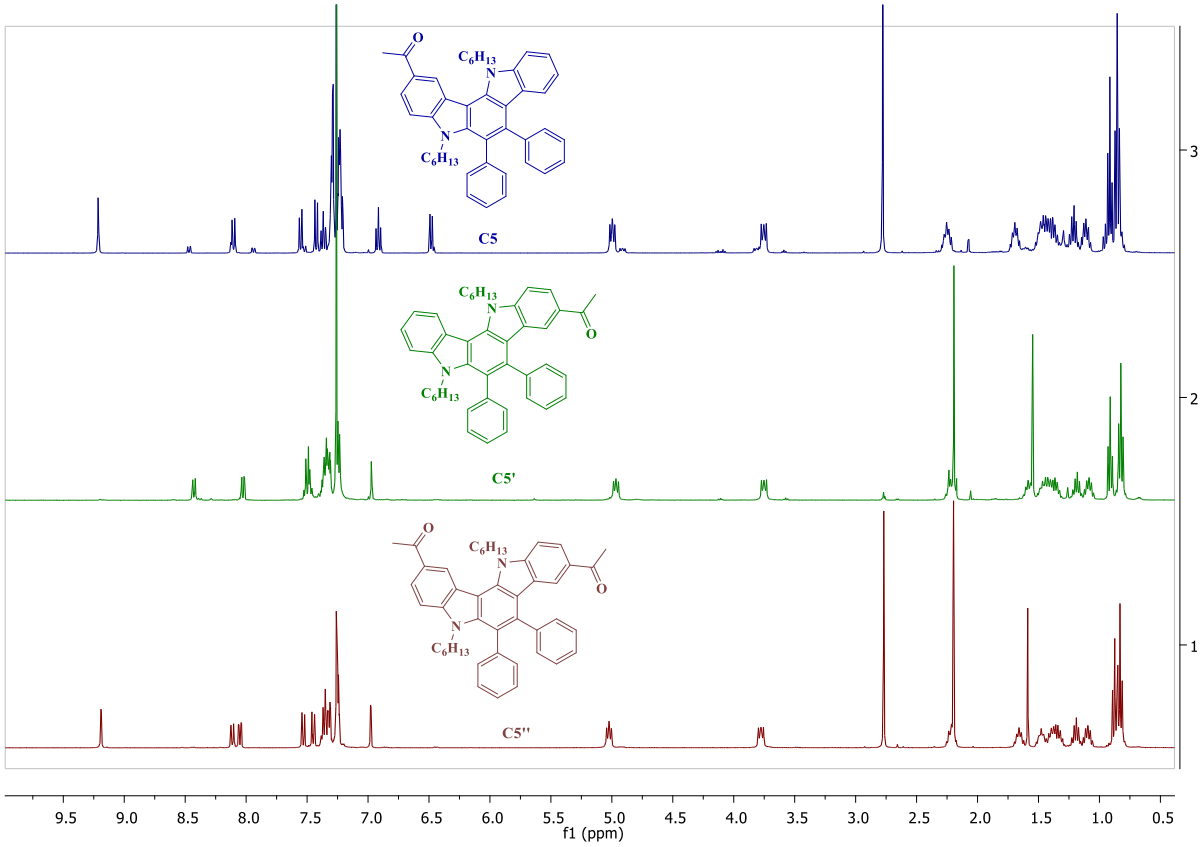

Figure 3. ^{1}H NMR spectra of **C5**, **C5'** and **C5''** recorded in chloroform.

Similarly, by use of one equivalent of HNO_3 65% and by stirring the solution at room temperature overnight, **C6** could be obtained in 52% yield. Interestingly, the nitro-derivative could be easily separated from **C2** by precipitation in diethyl ether, providing **C6** as an orange powder. All attempts to improve the reaction by elongating the reaction time or by slightly increasing the number of equivalents of HNO_3 65% only produced *the* bis-functionalized compound **C6'**. Considering that **C6** could be obtained in reasonable yield and that its colour was indicative of a strong absorption in the visible range, the introduction of functional groups

that could be later used for generating push-pull dyes or Suzuki cross-coupling reaction was examined. Thus, attempt to perform a Friedel-Craft reaction with acetyl chloride did not provide the targeted product **C7** and only a mixture of compounds that could not be separated was obtained. Similarly, the Rieche method ($SnCl_4$, 1,1-dichloromethyl methyl ether) applied on **C6** only furnished after treatment the initial product **C6**. Conversely, the Vilsmeier-Haack reaction applied to **C6** could provide **C8** in 72% yield after five days of reflux in chloroform (See Scheme 2). Halogenation of **C6** was also examined. Thus, bromination of **C6** with one equivalent of *N*-bromosuccinimide furnished **C9** in 96% yield respectively. Similarly, by using *N*-iodosuccinimide, **C10** could be obtained in 88% yield. Interestingly, all attempts to convert **C9** as **C8** using the standard procedure *n*-BuLi/DMF failed.

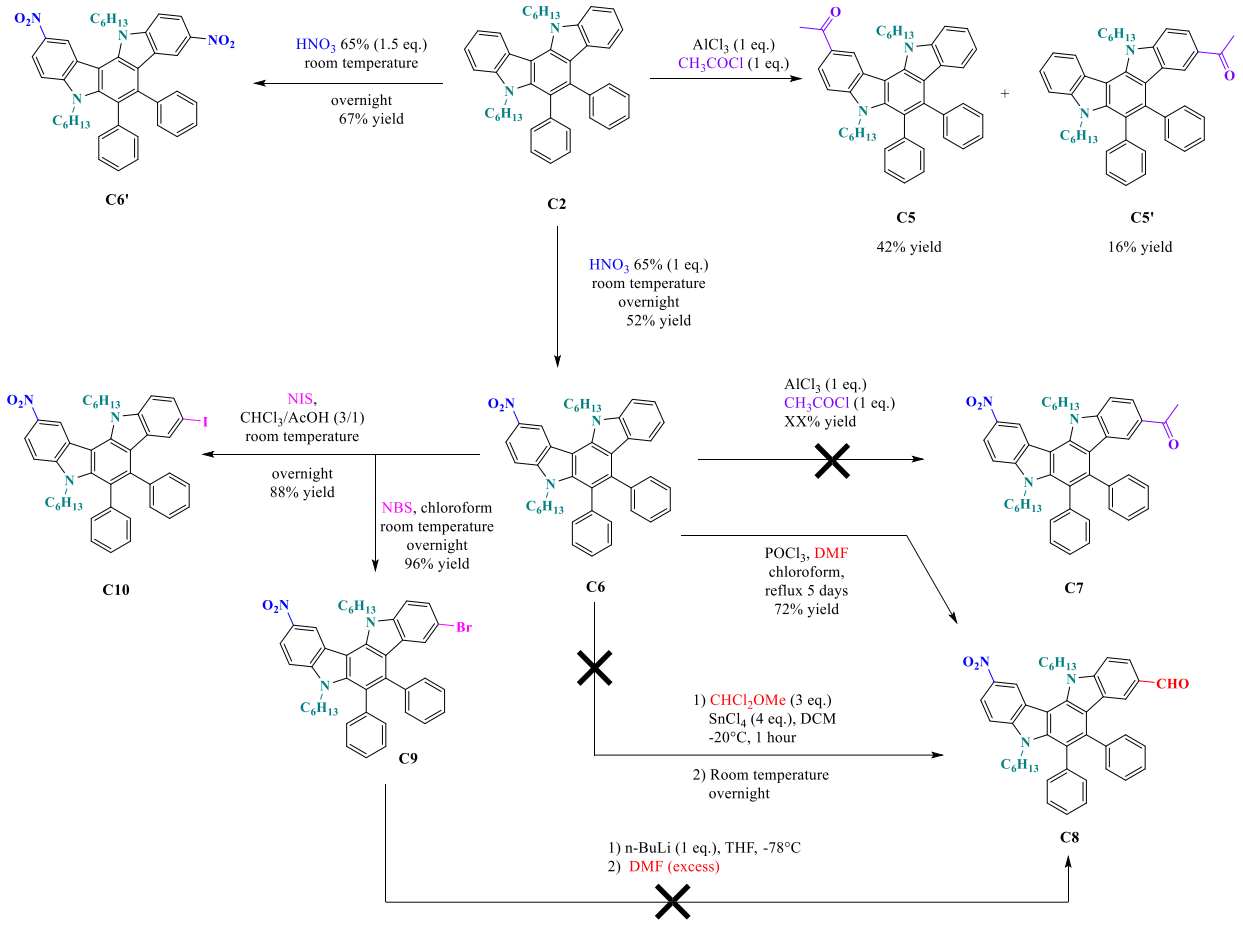

Scheme 2. Synthetic routes to **C5-C10**.

With aim at developing dyes strongly absorbing in the visible range with **C8**, push-pull dyes which consist in connecting a strong electron donor to an electron acceptor by mean of a π-conjugated spacer was examined. Especially, these dyes exhibit an intense absorption band corresponding to the intramolecular charge transfer band so that these dyes can be advantageously used as visible light photoinitiators of polymerization. Even if numerous

electron acceptors exist, only benchmark acceptors were examined in this study, namely, indane-1,3-dione, 1,3-dimethylbarbituric acid and 1,3-diethylthiobarbituric acid. The different Knoevenagel reactions could be carried out using ethanol as the solvent and piperidine as the catalyst. However, it has to be noticed that contrarily to the classical conditions of Knoevenagel reactions consisting in introducing both the aldehyde and the electron accepting group in stoichiometric conditions, three equivalents of electron accepting group had to be used in order to improve the reaction yield. Similar, a large excess of base had to be used and the reaction had to be maintained at reflux overnight. Using this procedure, all dyes **C11-C13** could be prepared with reaction yields ranging from 67% for **C13** to 88% for **C12** respectively (See Scheme 3).

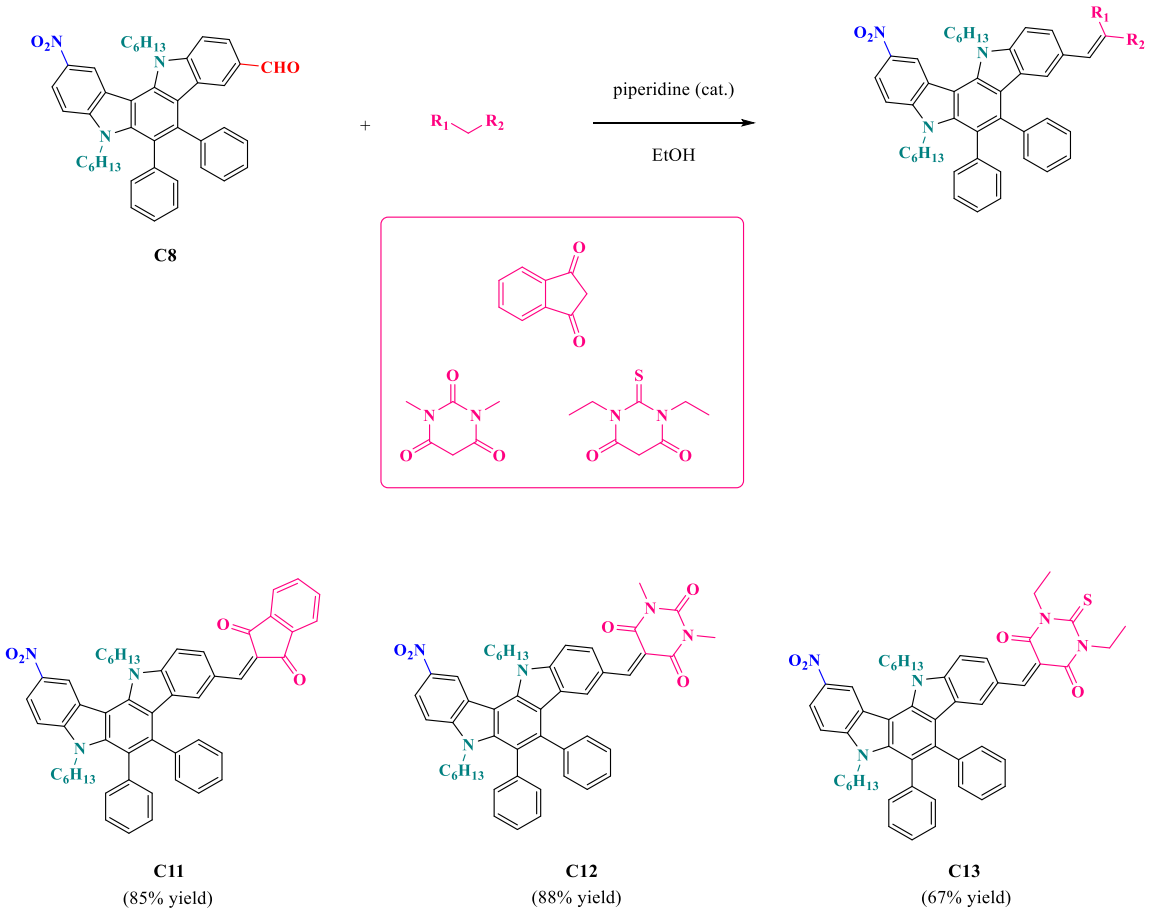

Scheme 3. Chemical structures of push-pull dyes **C11-C13** prepared with **C8** as the electron donor.

2.2. Other Chemicals compounds

Bis-(4-*tert*-butylphenyl)iodonium hexafluorophosphate (Iod; SpeedCure 938) was obtained from Lambson Ltd (UK). The monomers ((3,4-epoxycyclohexane)methyl 3,4-epoxycyclohexylcarboxylate (EPOX) and di(trimethylolpropane)tetraacrylate (TA)) were

obtained from Allnex. Chemical structures of monomers and additives are shown in the Scheme 4.

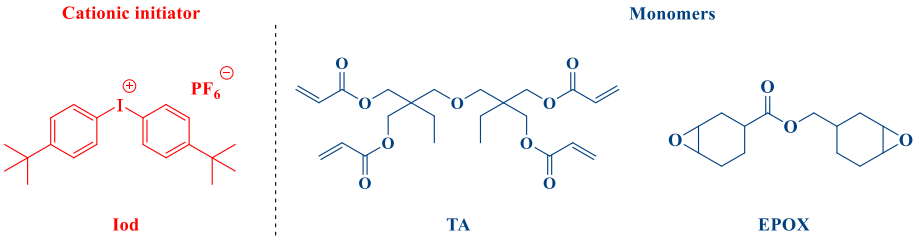

Scheme 4. Chemical structures of monomers and additives used in this study.

2.3. Irradiation Source

The following light-emitting diode (LED) was used as the irradiation source: LED@405 nm with an incident light intensity at the sample surface: I_0 = 110 mW.cm^{-2}.

2.4. UV-visible absorption and photolysis experiments

The UV-visible absorption properties of the different compounds as well as the steady state photolysis experiments were studied using a JASCO V730 UV-visible spectrometer.

2.5. Photopolymerization kinetics (RT-FTIR)

The experimental conditions for each photosensitive formulation are indicated in the caption of the figures. All the polymerizations were performed at room temperature and the irradiation was started at t = 10 s. The weight content of the photoinitiating system is calculated from the monomer content. The photoinitiator concentrations in each photosensitive formulation have been chosen to ensure good light absorption at 405 nm. The conversion of the acrylate functions of TA and the epoxide functions of EPOX were continuously followed by real time FTIR spectroscopy (JASCO FTIR 4100). For the thin samples (~25 µm of thickness), the photosensitive formulations were deposited on polypropylene films under air for the cationic polymerizations of EPOX while the free radical polymerizations of TMPTA were performed in laminate (the formulation is sandwiched between two polypropylene films to reduce the O_2 inhibition). The decrease of C=C double bond band or the epoxide group was continuously monitored from 1581 to 1662 cm^{-1} or from 768 to 825 cm^{-1} respectively. For the thicker samples (~1.4 mm of thickness), the formulations were deposited on a polypropylene film inside a 1.4 mm mold under air. The evolution of the C=C band and the epoxide group band were continuously followed from 6117 to 6221 cm^{-1} and from 3710 to 3799 cm^{-1} respectively.

2.6. Steady state fluorescence

Fluorescence spectra were acquired in a quartz cell at room temperature using a JASCO FP-750 spectrofluorometer.

2.7. Redox potentials

The redox potentials (E_{ox} and E_{red}) were measured in acetonitrile by cyclic voltammetry using tetrabutylammonium hexafluorophosphate (0.1 M) as the supporting electrolyte (potential vs. Saturated Calomel Electrode – SCE). The free energy change ΔG_{et} for an electron transfer reaction was calculated from eqn (1), [29] where E_{ox}, E_{red}, E*, and C are the oxidation potential of the electron donor, the reduction potential of the electron acceptor, the excited state energy and the coulombic term for the initially formed ion pair, respectively. Here, C is neglected for polar solvents.

$$\Delta G_{et} = E_{ox} - E_{red} - E^* + C \qquad \text{(Eqn. 1)}$$

2.8. Direct Laser Write

For direct laser write experiments, a laser diode emitting at 405 nm (spot size around 50 μm) was used for the spatially controlled irradiation. The photosensitive resin was polymerized under air and the generated 3D patterns were analyzed using a numerical optical microscope (DSX-HRSU from Olympus Corporation).

3. Results and discussion

3.1. UV-visible absorption properties of the different dyes

Among all compounds reported in this work, except **C2** which exhibits a UV-centred absorption (λ_{max} = 370 nm), all dyes showed absorption spectra extending until the visible range, making these dyes suitable candidates for photopolymerization experiments done under visible light. As shown in the Figure 4, three groups of dyes could be identified. First, dyes such as **C2, C3, C4, C5, C5'** and **C5''** proved to exhibit a strongly UV centred absorption so that only an onset could be detected in the visible range. As specificity, these dyes are substituted with weak electron accepting groups such as aldehyde and acetyl groups.

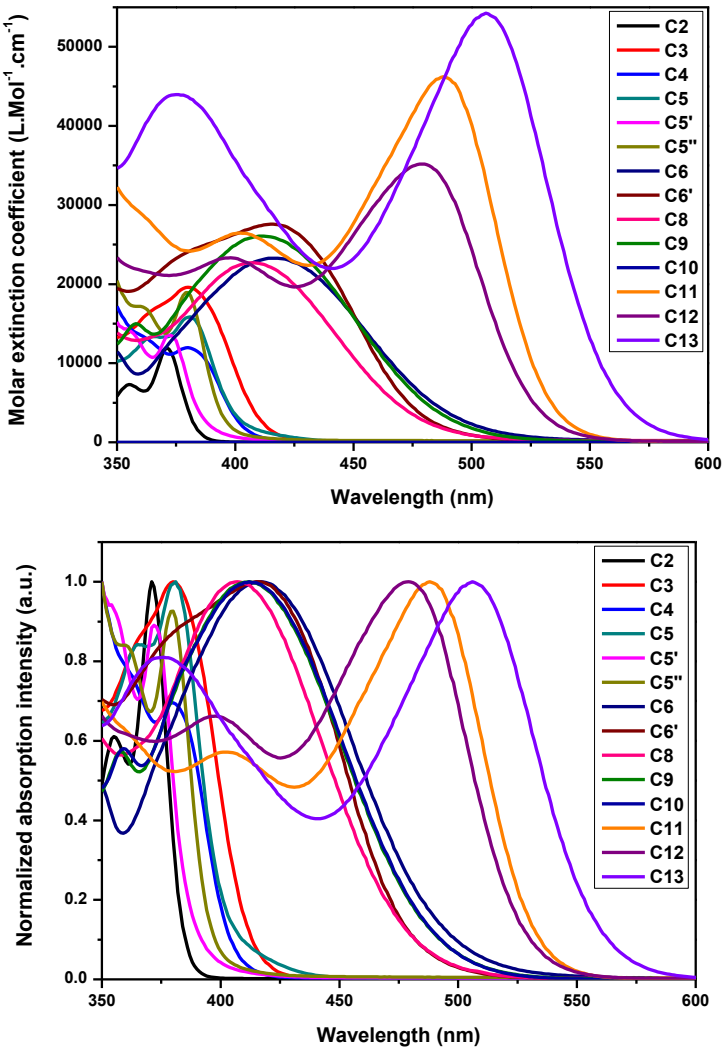

Figure 4. UV visible absorption spectra of different dyes in chloroform. top: molar extinction coefficient. bottom: normalized absorption.

Conversely, for all dyes substituted with a nitro group i.e. **C6, C6', C8** and **C8**, absorption maxima ranging from 408 nm for **C8** to 417 nm for **C6** and **C6'** could be determined. Interestingly, contrarily to **C6** and **C6'** that are only substituted with one or two nitro groups, introduction of additional groups such as a bromine on **C9**, an iodine on **C10** or an aldehyde on **C8** slightly blue-shifted their absorption maxima compared to the parent structure **C6**. Finally, by converting **C8** as an electron donating group for push-pull dyes, a major redshift of the absorption maxima could be determined. Thus, the absorption maxima of **C11-C13** could be determined respectively at 488, 479 and 505 nm. Interestingly, even if a stronger electron-withdrawing group was used in **C12** compared to **C11**, a hypsochromic shift of the absorption maxima of ca. 10 nm could be determined. This unexpected result can be assigned to the steric hindrance existing between the phenyl groups of the electron donor with the 6-membered ring of the electron acceptor in **C12**, enforcing the π-conjugated system to twist. Conversely, a more

planar structure can be obtained in **C11**, due to the presence of an electron accepting group bearing a five-membered ring.

Table 1. Optical characteristics of different dyes in chloroform as the solvent.

compounds	**C2**	**C3**	**C4**	**C5**	**C5'**	**C5''**	**C6**
λ (nm)	370	380	379	380	372	380	417
ε ($M^{-1}.cm^{-1}$)	12000	19500	11800	15900	13500	18800	23500
compounds	**C6'**	**C8**	**C9**	**C10**	**C11**	**C12**	**C13**
λ (nm)	417	408	412	412	489	479	505
ε ($M^{-1}.cm^{-1}$)	27500	22700	25900	17400	42600	34900	54100

3.2. Photopolymerization abilities of the different dyes

3.2.1. Free radical polymerization (FRP) of acrylates

For the polymerization of the acrylate monomer TA, the photoinitiation abilities of the different dyes in the presence of an iodonium salt as the additive were investigated using real-time Fourier transform infrared spectroscopy (RT-FTIR) upon irradiation with LED@405 nm at room temperature. Typical acrylate function conversions vs. irradiation time profiles are given in Figure 5 and the associated final acrylate function conversions (FCs) are summarized in Table 2.

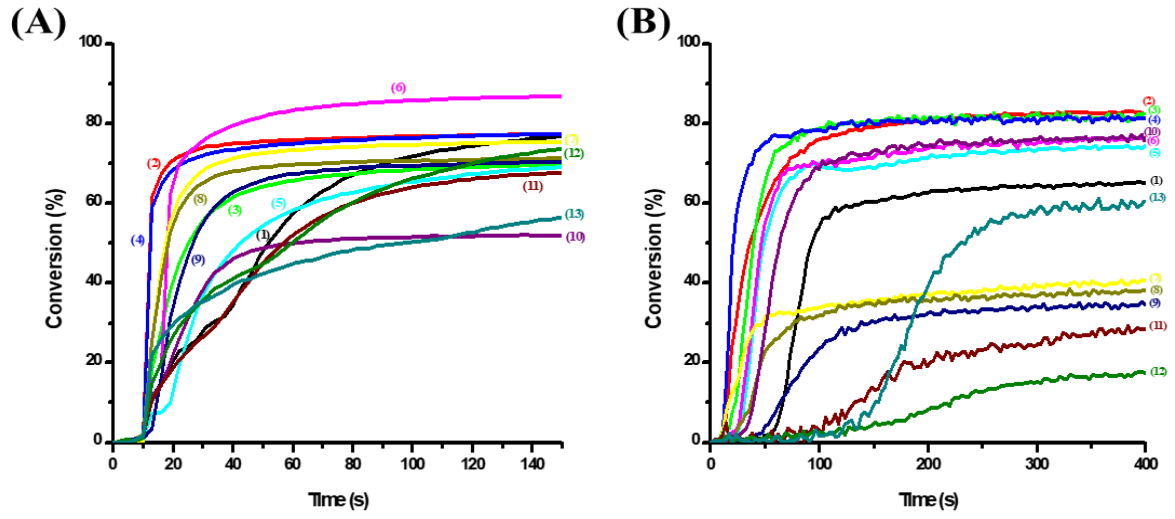

Figure 5. (A) Polymerization profiles of TA (acrylate function conversion vs. irradiation time) in laminate (thickness = 25 μm) upon exposure to LED light λ = 405 nm in the presence of two-component photoinitiating systems: (1) **C2**/Iod (0.2%/1% w/w); (2) **C3**/Iod (0.2%/1% w/w); (3) **C4**/Iod (0.2%/1% w/w); (4) **C5**/Iod (0.2%/1% w/w); (5) **C5'**/Iod (0.2%/1% w/w); (6) **C5''**/Iod (0.2%/1% w/w); (7) **C6**/Iod (0.2%/1% w/w); (8) **C6'**/Iod (0.2%/1% w/w); (9) **C8**/Iod (0.2%/1% w/w); (10) **C9**/Iod (0.2%/1% w/w); (11) **C11**/Iod (0.2%/1% w/w); (12) **C12**/Iod (0.2%/1% w/w); and (13) **C13**/Iod (0.2%/1% w/w);

respectively. The irradiation starts at t = 10 s. (B) Polymerization profiles of TA (acrylate function conversion vs. irradiation time) under air (thickness = 1.4 mm) upon exposure to LED light λ=405 nm in the presence of two-component photoinitiating systems: (1) **C2**/Iod (0.2%/1% w/w); (2) **C3**/Iod (0.2%/1% w/w); (3) **C4**/Iod (0.2%/1% w/w); (4) **C5**/Iod (0.2%/1% w/w); (5) **C5'**/Iod (0.2%/1% w/w); (6) **C5''**/Iod (0.2%/1% w/w); (7) **C6**/Iod (0.2%/1% w/w); (8) **C6'**/Iod (0.2%/1% w/w); (9) **C8**/Iod (0.2%/1% w/w); (10) **C9**/Iod (0.2%/1% w/w); (11) **C11**/Iod (0.2%/1% w/w); (12) **C12**/Iod (0.2%/1% w/w); and (13) **C13**/Iod (0.2%/1% w/w); respectively. The irradiation starts at t = 10 s.

Table 2. Final acrylate function conversion (FCs) for TA using Dyes/Iod (0.2%/1% w/w) as photoinitiating systems, after 100 s of irradiation with the LED emitting at 405 nm.

	Thin sample (25 µm) in laminate	**Thick sample (1.4 mm) under air**
	PI/Iod (0.2%/1% w/w)	PI/Iod (0.2%/1% w/w)
C2	77%	66%
C3	77%	83%
C4	70%	82%
C5	77%	81%
C5'	69%	75%
C5''	87%	76%
C6	75%	40%
C6'	71%	38%
C8	70%	34%
C9	52%	77%
C11	68%	28%
C12	74%	17%
C13	56%	61%

Upon exposure to LED irradiation at 405 nm, the experimental results showed that almost all dyes, when combined with an iodonium salt, can effectively initiate free radical polymerizations (e.g. FC= 87% with 0.2% **C5''** (w/w) and FC= 77% with 0.2% **C2**, or **C3** or **C5** (w/w) for thin sample (25µm, in laminate); Figure 5 (A), Table 2). For dyes alone, no polymerization is

observed showing the interest of the two-component systems. The efficiency trend for dyes/Iod couples for the FRP in thin samples (25 µm, in laminate) respects the following order: **C5'' > C2 ~ C3 ~ C5 > C6 > C12 > C6' > C4 ~ C8 > C5' > C11 > C13 > C9** which is not directly related to the absorption properties of the different dyes, but also to the photochemical reactivity with the iodonium salt and also probably by the different reactivity of the generated radicals to initiate the free radical polymerization. For thick samples (1.4 mm, under air), the dye/Iod systems also showed high final acrylic conversions, but for some dyes (e.g., **C12** and **C13**) the polymerization was low compared to the results obtained in thin samples. This behaviour can be attributed to an internal filter effect (See Figure 5 (B), Table 2).

3.2.2. Cationic polymerization (CP) of epoxides

The investigated dyes were also tested as photosensitizers for the iodonium salt (Iod) in the cationic polymerization (CP) of EPOX upon irradiation with a LED@405 nm. Epoxy function conversion versus irradiation time profiles are shown in Figure 6 and the associated final epoxy function conversions (FC's) are gathered in Table 3. For Iod alone in EPOX, no polymerization occurs in agreement with the lack of absorption of the iodonium salt at 405 nm.

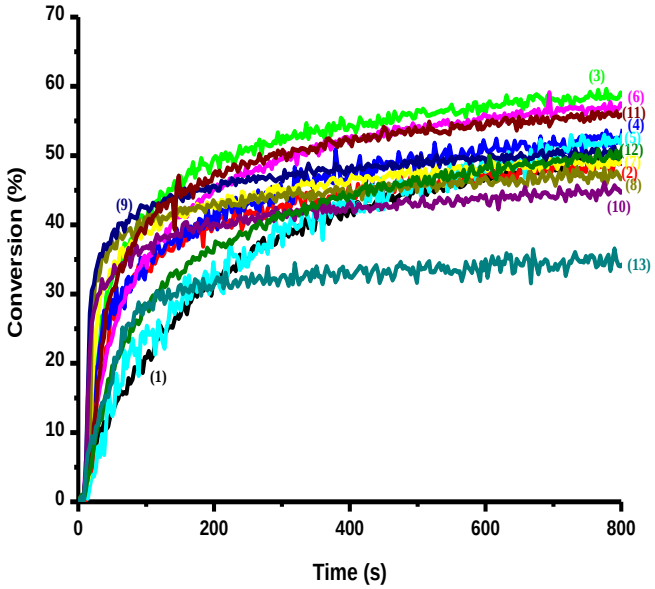

Figure 6. Photopolymerization profiles of EPOX (epoxy function conversion vs. irradiation time) under air (thickness= 25 µm) upon exposure to LED light λ= 405 nm in the presence of different two component photoinitiating systems: PI/Iod (0.2%/1% w/w): (1) **C2**/Iod; (2) **C3**/Iod; (3) **C4**/Iod; (4) **C5**/Iod; (5) **C5'**/Iod; (6) **C5''**/Iod; (7) **C6**/Iod; (8) **C6'**/Iod; (9) **C8**/Iod; (10) **C9**/Iod; (11) **C11**/Iod; (12) **C12**/Iod; and (13) **C13**/Iod; respectively. The irradiation starts after t = 10 s.

Table 3. Final epoxy function conversions (FCs) for EPOX using different two-component dyes/Iod (0.2%/1% w/w) photoinitiating systems after 800 s of irradiation with LED light (λ = 405 nm).

Thin sample (25 µm) in laminate												
C2	**C3**	**C4**	**C5**	**C5'**	**C5''**	**C6**	**C6'**	**C8**	**C9**	**C11**	**C12**	**C13**
50%	49%	59%	54%	53%	57%	49%	47%	51%	45%	56%	51%	34%

Actually, the different dyes can efficiently absorb the light at 405 nm, and then the corresponding generated excited states are expected to interact with the iodonium salt as a photoinitiator in order to generate reactive species ($Dye^{\bullet+}$; see reactions r1 and r2 below), which are able to initiate the cationic polymerization of thin (25 µm) epoxy films as shown in the Figure 6. The two-component dyes/Iod (0.2%/1% w/w) photoinitiating systems are very efficient to initiate the CP under air where very high final functional conversions (FCs) and also high rates of polymerization (Rp) were achieved i.e., FC= 57% for **C5''**/Iod (0.2%/1% w/w) (curve 6 in Figure 6; see also in Table 3 for the other dyes). The efficiency trend for dyes/Iod couples for the CP respects the following order: **C4** > **C5''** > **C11** > **C5** > C**5'** > C**8** ~ **C12** > **C2** > **C3** ~ **C6** > **C6'** > **C9** > **C13** which also is not directly linked to the absorption properties of the investigated dyes. Therefore, the photochemical reactivity with the iodonium salt is probably affected by the dye structure and also probably different reactivity of the generated radical cations ($Dye^{\bullet+}$) to initiate the CP. Interestingly, comparisons of the EPOX conversions obtained in this work for **C5''** and **C11** with results previously reported in the literature for carbazole-based structures revealed **C5''** and **C11** to furnish similar conversions at 405 nm to that obtained with the three-component carbazole/NVK/Ph_2I^+ (0.3%/3%/2% w/w) photoinitiating systems comprising **Carb_1** (55%) [53] or **Carb_2** (58%).[54] If **C5''** and **C11** can compete the two-component carbazole/(*t*-Bu)Ph_2I^+ (0.2%/2% w/w) photoinitiating systems based on **Carb_4** (50%) and **Carb_5** (58%), the EPOX conversions were lower than that obtained with other nitrated carbazoles such as **Carb_3** (76%) and **Carb_6** (70%).[32] However, EPOX conversions obtained with **C5''** and **C11** remain comparable to that of **Carb_7** (57 % yield) [29] (See Figure 7).

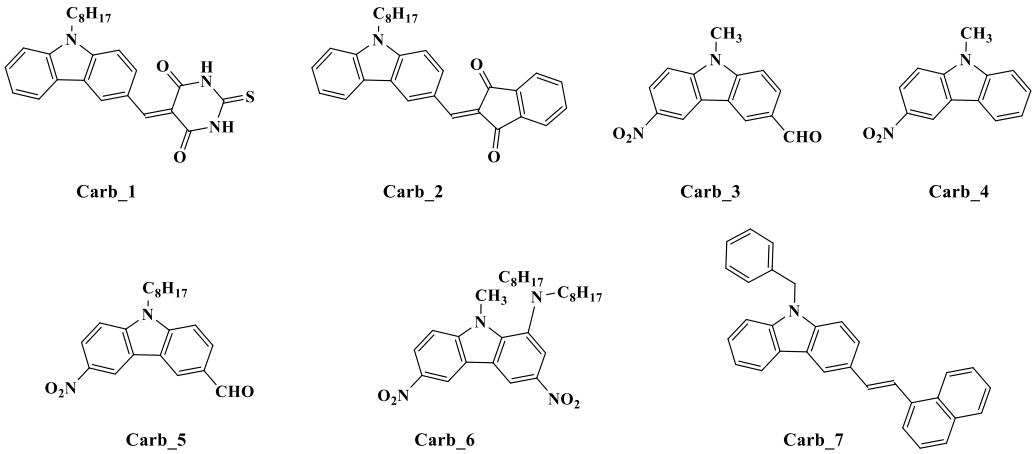

Figure 7. Chemical structures of carbazole derivatives previously used as visible photoinitiators of polymerization for the cationic polymerization of EPOX.

3.3. Chemical mechanisms

3.3.1. Steady state photolysis

Steady-state photolysis of the dyes/Iod (10^{-2} M) systems is performed in acetonitrile under light irradiation, using an LED@375 nm. It is remarkable that, for example for **C5''** (Figure 7 (A)), there is an efficient photolysis with the rapid formation of photoproducts after 40 s, and for **C6'** after 1920 s (Figure 7 (B)), which may suggest a photochemical reaction between the studied dyes and the iodonium salt, in agreement with the results observed in the photopolymerization experiments. Isobestic points were observed suggesting photochemical processes without side-reactions.

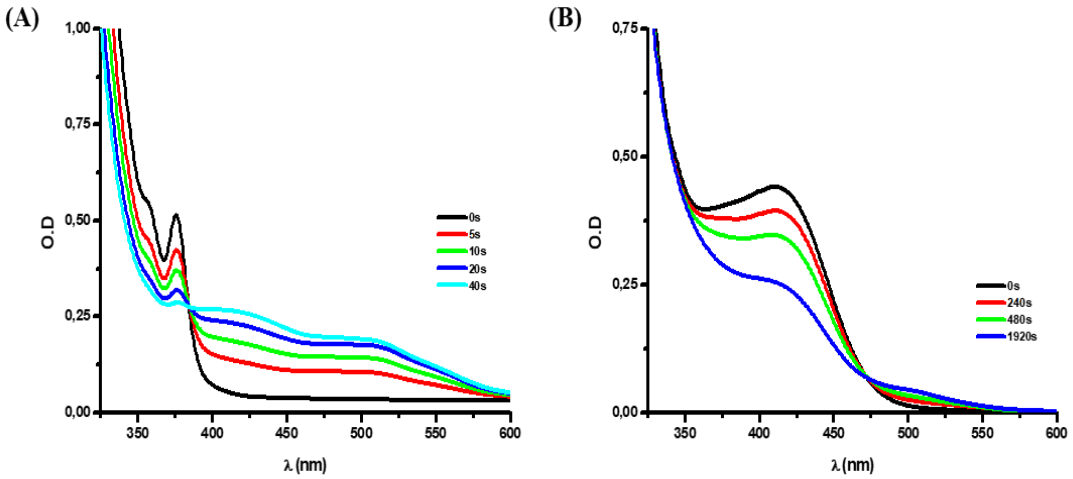

Figure 7. (A) Photolysis of **C5''** with Iod (10^{-2} M) in acetonitrile; (B) Photolysis of **C6'** with Iod (10^{-2} M) in acetonitrile.

3.3.2. Fluorescence quenching

In order to better understand the interaction between the studied dyes and the iodonium salt (Iod), fluorescence quenching experiments were carried out. For example, as Figure 4 shows, a strong fluorescence quenching process of **C2** by Iod was detected (see Figure 8 and Table 4); this clearly shows a very strong interaction of **C2** (and even the other dyes) with the iodonium salt ((r1) and (r2)). The oxidation potentials (E_{ox}) determined by cyclic voltammetry (Table 4) allow the evaluation of the free energy change (ΔG) for this electron transfer reaction (Table 4); highly favorable ΔG are found in agreement with the strong ^{1}**C2**/Iod interaction observed above in fluorescence quenching. The associated electron transfer quantum yields (Φ_{et}) were determined according to the following equation: $\Phi_{et} = ksv[Iod]/(1 + ksv[Iod])$ and high Φ_{et} are found (e.g., $\Phi = 0.79$ for **C2**, Table 4).

$$Dye\ (h\nu) \rightarrow {}^{*}Dye \qquad (r1)$$

$$^{*}Dye + Ar_2I^{+} \rightarrow Dye^{\bullet+} + Ar_2I^{\bullet} \rightarrow Dye^{\bullet+} + Ar^{\bullet} + ArI \qquad (r2)$$

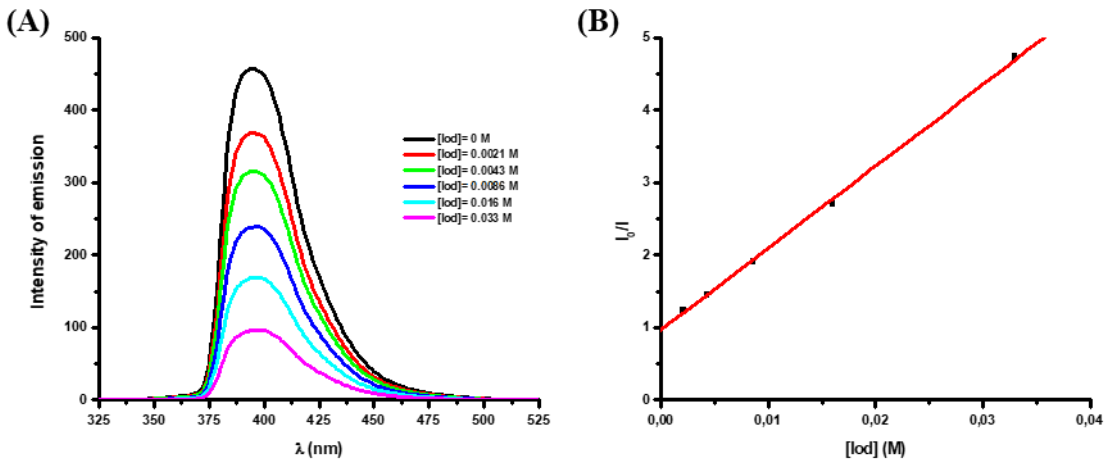

Figure 8. (A) Quenching of ^{1}**C2** by Iod in acetonitrile. (B) Determination of the Stern-Volmer coefficient.

Table 4. Parameters characterizing the chemical mechanisms associated with ^{1}dyes/Iod interaction in acetonitrile.

PI	E_{ox} (eV)	E_{S1} (eV)	$\Delta G_{S1\ (Iod)}$ (eV)[a]	K_{sv} (M^{-1})[b]	$\Phi_{et(Dye/Iod)}$

C2	0.88	3.28	-1.7	113	0.79
C3	1.04	3.04	-1.3	99	0.61
C4	1.17	3.11	-1.24	82	0.55
C5	1.01	3.10	-1.39	245	0.78
C5'	0.95	3.23	-1.58	18	0.21
C5''	1.12	3.19	-1.37	76	0.68
C6	1.11	-	-	-	-
C6'	1.15	-	-	-	-
C8	1.24	-	-	-	-
C9	1.19	-	-	-	-
C11	1.22	-	-	-	-
C12	1.21	-	-	-	-
C13	1.21	-	-	-	-

a: evaluated from $\Delta G_{S1} = E_{ox} - E_{red}(Iod) - E_{S1}$; $E_{red}(Iod) = -0.7$ V.

b: Stern-Volmer coefficient (K_{sv}); slope of the quenching curve: $I/I_0=(1+ksv[Iod])$.

3.4. 3D printing experiment

Some 3D printing experiments upon laser diode irradiation at 405 nm were successfully performed under air using **C4**/Iod and **C5**/Iod systems in TA (See Figure 9). Indeed, the high photosensibility of these systems allows an efficient polymerization in the irradiated area. 3D patterns elaborated with high resolution and very short writing time (~ 2 min), were characterized by numerical optical microscopy.

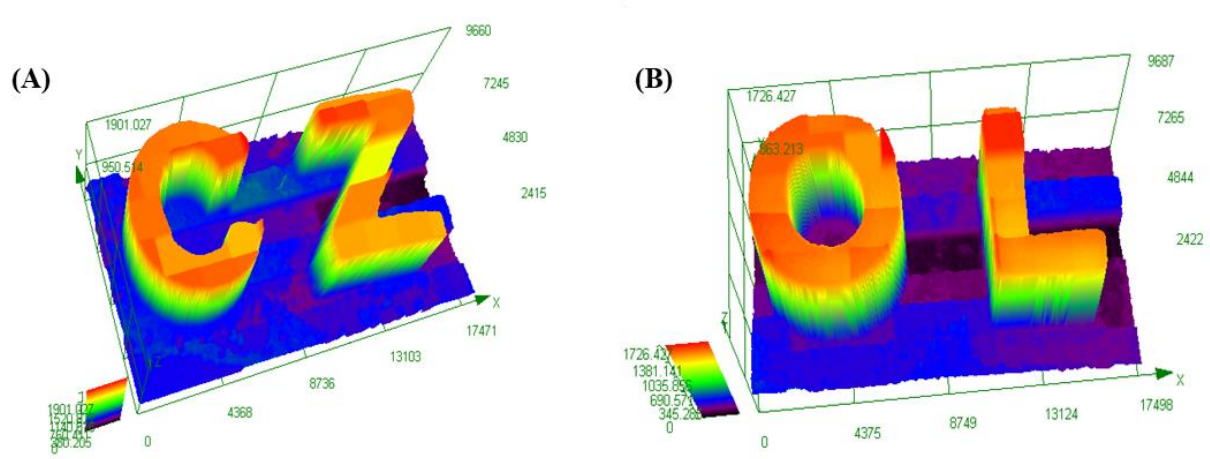

Figure 9. 3D patterns obtained upon exposure to a laser diode @405 nm: characterization by numerical microscopy; (A): **C4**/Iod (0.2%/1% w/w) in TA (thickness= 1900 µm); (B): **C5**/Iod (0.2%/1% w/w/) in TA (thickness= 1700 µm).

5. Conclusion

In the present paper, a series of 5,12-dihydroindolo[3,2-a]carbazole derivatives characterized by strong visible light absorptions in the visible range are proposed for the development of new high performance photoinitiators for both the free radical polymerization of acrylates and the cationic polymerization of epoxides upon blue LED irradiation. Both high final conversions and polymerization rates are achieved. The high performance of these proposed dyes in initiating systems is also shown for new photosensitive 3D printing resins upon exposure to a laser diode. The challenge remains, therefore, to develop new photoinitiating systems absorbing at longer wavelengths for example in the near-infrared range for a better penetration of light into thick samples.

Acknowledgments

Aix Marseille University and the Centre National de la Recherche Scientifique (CNRS) are acknowledged for financial supports.

Conflicts of Interest

The authors declare no conflict of interest.

References

[1] K.L. Woon, A. Ariffin, K.W. Ho, S.-A. Chen, Effect of conjugation and aromaticity of 3,6 di-substituted carbazoles on triplet energy and the implication of triplet energy in multiple-cyclic aromatic compounds, RSC Adv. 8 (2018) 9850–9857. https://doi.org/10.1039/C8RA00674A.

[2] A. Arai, H. Sasabe, K. Nakao, Y. Masuda, J. Kido, π-Extended Carbazole Derivatives as Host Materials for Highly Efficient and Long-Life Green Phosphorescent Organic Light-Emitting Diodes, Chemistry – A European Journal. 27 (2021) 4971–4976. https://doi.org/10.1002/chem.202005144.

[3] Y. Nagai, H. Sasabe, S. Ohisa, J. Kido, Effect of substituents in a series of carbazole-based host-materials toward high-efficiency carbene-based blue OLEDs, J. Mater. Chem. C. 4 (2016) 9476–9481. https://doi.org/10.1039/C6TC03067J.

[4] Z.-J. Gao, T.-H. Yeh, J.-J. Xu, C.-C. Lee, A. Chowdhury, B.-C. Wang, S.-W. Liu, C.-H. Chen, Carbazole/Benzimidazole-Based Bipolar Molecules as the Hosts for Phosphorescent and Thermally Activated Delayed Fluorescence Emitters for Efficient OLEDs, ACS Omega. 5 (2020) 10553–10561. https://doi.org/10.1021/acsomega.0c00967.

[5] G. Li, J. Zheng, K. Klimes, Z.-Q. Zhu, J. Wu, H. Zhu, J. Li, Novel Carbazole/Fluorene-Based Host Material for Stable and Efficient Phosphorescent OLEDs, ACS Appl. Mater. Interfaces. 11 (2019) 40320–40331. https://doi.org/10.1021/acsami.9b13245.

[6] F. Dumur, Carbazole-based polymers as hosts for solution-processed organic light-emitting diodes: Simplicity, efficacy, Organic Electronics. 25 (2015) 345–361. https://doi.org/10.1016/j.orgel.2015.07.007.

[7] F. Dumur, L. Beouch, S. Peralta, G. Wantz, F. Goubard, D. Gigmes, Solution-processed blue phosphorescent OLEDs with carbazole-based polymeric host materials, Organic Electronics. 25 (2015) 21–30. https://doi.org/10.1016/j.orgel.2015.06.013.

[8] G. Sathiyan, E.K.T. Sivakumar, R. Ganesamoorthy, R. Thangamuthu, P. Sakthivel, Review of carbazole based conjugated molecules for highly efficient organic solar cell application, Tetrahedron Letters. 57 (2016) 243–252. https://doi.org/10.1016/j.tetlet.2015.12.057.

[9] I.V. Martynov, A.V. Akkuratov, S.Yu. Luchkin, S.A. Tsarev, S.D. Babenko, V.G. Petrov, K.J. Stevenson, P.A. Troshin, Impressive Radiation Stability of Organic Solar Cells Based on Fullerene Derivatives and Carbazole-Containing Conjugated Polymers, ACS Appl. Mater. Interfaces. 11 (2019) 21741–21748. https://doi.org/10.1021/acsami.9b01729.

[10] J. Ouyang, G. Zeng, Y. Xin, X. Zhao, X. Yang, A Novel Carbazole-Based Nonfullerene Acceptor for High-Efficiency Polymer Solar Cells, Solar RRL. 4 (2020) 1900417. https://doi.org/10.1002/solr.201900417.

[11] B. Souharce, C.J. Kudla, M. Forster, J. Steiger, R. Anselmann, H. Thiem, U. Scherf, Amorphous Carbazole-based (Co)polymers for OFET Application, Macromolecular Rapid Communications. 30 (2009) 1258–1262. https://doi.org/10.1002/marc.200900214.

[12] P. Jha, S.P. Koiry, V. Saxena, P. Veerender, A. Gusain, A.K. Chauhan, A.K. Debnath, D.K. Aswal, S.K. Gupta, Air-stability and bending properties of flexible organic field-effect transistors based on poly[N-9′-heptadecanyl-2,7-carbazole-alt-5,5-(4′,7′-di-2-thienyl-2′,1′,3′-benzothiadiazole)], Organic Electronics. 14 (2013) 2635–2644. https://doi.org/10.1016/j.orgel.2013.06.031.

[13] C.-H. Chen, Y. Wang, T. Michinobu, S.-W. Chang, Y.-C. Chiu, C.-Y. Ke, G.-S. Liou, Donor–Acceptor Effect of Carbazole-Based Conjugated Polymer Electrets on Photoresponsive Flash Organic Field-Effect Transistor Memories, ACS Appl. Mater. Interfaces. 12 (2020) 6144–6150. https://doi.org/10.1021/acsami.9b20960.

[14] M. Khalid, A. Ali, R. Jawaria, M.A. Asghar, S. Asim, M.U. Khan, R. Hussain, M.F. ur Rehman, C.J. Ennis, M.S. Akram, First principles study of electronic and nonlinear optical properties of A–D–

π–A and D–A–D–π–A configured compounds containing novel quinoline–carbazole derivatives, RSC Adv. 10 (2020) 22273–22283. https://doi.org/10.1039/D0RA02857F.
[15] MayuriM.L. Kadam, D. Patil, N. Sekar, Fluorescent carbazole based pyridone dyes – Synthesis, solvatochromism, linear and nonlinear optical properties, Optical Materials. 85 (2018) 308–318. https://doi.org/10.1016/j.optmat.2018.08.072.
[16] W.-J. Kuo, G.-H. Hsiue, R.-J. Jeng, All Organic NLO Sol-Gel Material Containing a One-Dimensional Carbazole Chromophore, Macromolecular Chemistry and Physics. 202 (2001) 1782–1790. https://doi.org/10.1002/1521-3935(20010601)202:9<1782::AID-MACP1782>3.0.CO;2-O.
[17] M. Rajeshirke, M.C. Sreenath, S. Chitrambalam, I.H. Joe, N. Sekar, Enhancement of NLO Properties in OBO Fluorophores Derived from Carbazole–Coumarin Chalcones Containing Carboxylic Acid at the N-Alykl Terminal End, J. Phys. Chem. C. 122 (2018) 14313–14325. https://doi.org/10.1021/acs.jpcc.8b02937.
[18] M. Bashir, A. Bano, A.S. Ijaz, B.A. Chaudhary, Recent Developments and Biological Activities of N-Substituted Carbazole Derivatives: A Review, Molecules. 20 (2015) 13496–13517. https://doi.org/10.3390/molecules200813496.
[19] M. Lepeltier, F. Appaix, Y.Y. Liao, F. Dumur, J. Marrot, T. Le Bahers, C. Andraud, C. Monnereau, Carbazole-Substituted Iridium Complex as a Solid State Emitter for Two-Photon Intravital Imaging, Inorg. Chem. 55 (2016) 9586–9595. https://doi.org/10.1021/acs.inorgchem.6b01253.
[20] F. Dumur, Recent advances on carbazole-based photoinitiators of polymerization, European Polymer Journal. 125 (2020) 109503. https://doi.org/10.1016/j.eurpolymj.2020.109503.
[21] N. Blouin, A. Michaud, D. Gendron, S. Wakim, E. Blair, R. Neagu-Plesu, M. Belletête, G. Durocher, Y. Tao, M. Leclerc, Toward a Rational Design of Poly(2,7-Carbazole) Derivatives for Solar Cells, J. Am. Chem. Soc. 130 (2008) 732–742. https://doi.org/10.1021/ja0771989.
[22] K.H. Choi, J.M. Kim, W.J. Chung, J.Y. Lee, Effects of Substitution Position of Carbazole-Dibenzofuran Based High Triplet Energy Hosts to Device Stability of Blue Phosphorescent Organic Light-Emitting Diodes, Molecules. 26 (2021) 2804. https://doi.org/10.3390/molecules26092804.
[23] A. van Dijken, J.J.A.M. Bastiaansen, N.M.M. Kiggen, B.M.W. Langeveld, C. Rothe, A. Monkman, I. Bach, P. Stössel, K. Brunner, Carbazole Compounds as Host Materials for Triplet Emitters in Organic Light-Emitting Diodes: Polymer Hosts for High-Efficiency Light-Emitting Diodes, J. Am. Chem. Soc. 126 (2004) 7718–7727. https://doi.org/10.1021/ja049771j.
[24] S.O. Jung, Y.-H. Kim, S.-K. Kwon, H.-Y. Oh, J.-H. Yang, New hole blocking material for green-emitting phosphorescent organic electroluminescent devices, Organic Electronics. 8 (2007) 349–356. https://doi.org/10.1016/j.orgel.2006.12.005.
[25] F. Dumur, D. Bertin, C.R. Mayer, A. Guerlin, G. Wantz, G. Nasr, E. Dumas, F. Miomandre, G. Clavier, D. Gigmes, Design of blue or yellow emitting devices controlled by the deposition process of a cationic iridium (III) complex, Synthetic Metals. 161 (2011) 1934–1939. https://doi.org/10.1016/j.synthmet.2011.06.038.
[26] D. Sun, Q. Fu, Z. Ren, W. Li, H. Li, D. Ma, S. Yan, Carbazole-based polysiloxane hosts for highly efficient solution-processed blue electrophosphorescent devices, J. Mater. Chem. C. 1 (2013) 5344–5350. https://doi.org/10.1039/C3TC31108B.
[27] J. Zhang, D. Campolo, F. Dumur, P. Xiao, D. Gigmes, J.P. Fouassier, J. Lalevée, The carbazole-bound ferrocenium salt as a specific cationic photoinitiator upon near-UV and visible LEDs (365–405 nm), Polym. Bull. 73 (2016) 493–507. https://doi.org/10.1007/s00289-015-1506-1.
[28] A. Al Mousawi, D.M. Lara, G. Noirbent, F. Dumur, J. Toufaily, T. Hamieh, T.-T. Bui, F. Goubard, B. Graff, D. Gigmes, J.P. Fouassier, J. Lalevée, Carbazole Derivatives with Thermally Activated Delayed Fluorescence Property as Photoinitiators/Photoredox Catalysts for LED 3D Printing Technology, Macromolecules. 50 (2017) 4913–4926. https://doi.org/10.1021/acs.macromol.7b01114.
[29] A. Al Mousawi, P. Garra, F. Dumur, T.-T. Bui, F. Goubard, J. Toufaily, T. Hamieh, B. Graff, D. Gigmes, J.P. Fouassier, J. Lalevée, Novel Carbazole Skeleton-Based Photoinitiators for LED

Polymerization and LED Projector 3D Printing, Molecules. 22 (2017) 2143. https://doi.org/10.3390/molecules22122143.
[30] A.A. Mousawi, A. Arar, M. Ibrahim-Ouali, S. Duval, F. Dumur, P. Garra, J. Toufaily, T. Hamieh, B. Graff, D. Gigmes, J.-P. Fouassier, J. Lalevée, Carbazole-based compounds as photoinitiators for free radical and cationic polymerization upon near visible light illumination, Photochem. Photobiol. Sci. 17 (2018) 578–585. https://doi.org/10.1039/C7PP00400A.
[31] M. Abdallah, D. Magaldi, A. Hijazi, B. Graff, F. Dumur, J.-P. Fouassier, T.-T. Bui, F. Goubard, J. Lalevée, Development of new high-performance visible light photoinitiators based on carbazole scaffold and their applications in 3d printing and photocomposite synthesis, Journal of Polymer Science Part A: Polymer Chemistry. 57 (2019) 2081–2092. https://doi.org/10.1002/pola.29471.
[32] A. Al Mousawi, F. Dumur, P. Garra, J. Toufaily, T. Hamieh, B. Graff, D. Gigmes, J.P. Fouassier, J. Lalevée, Carbazole Scaffold Based Photoinitiator/Photoredox Catalysts: Toward New High Performance Photoinitiating Systems and Application in LED Projector 3D Printing Resins, Macromolecules. 50 (2017) 2747–2758. https://doi.org/10.1021/acs.macromol.7b00210.
[33] S. Telitel, F. Dumur, T. Faury, B. Graff, M.-A. Tehfe, D. Gigmes, J.-P. Fouassier, J. Lalevée, New core-pyrene π structure organophotocatalysts usable as highly efficient photoinitiators, Beilstein J. Org. Chem. 9 (2013) 877–890. https://doi.org/10.3762/bjoc.9.101.
[34] A.A. Mousawi, F. Dumur, P. Garra, J. Toufaily, T. Hamieh, F. Goubard, T.-T. Bui, B. Graff, D. Gigmes, J.P. Fouassier, J. Lalevée, Azahelicenes as visible light photoinitiators for cationic and radical polymerization: Preparation of photoluminescent polymers and use in high performance LED projector 3D printing resins, Journal of Polymer Science Part A: Polymer Chemistry. 55 (2017) 1189–1199. https://doi.org/10.1002/pola.28476.
[35] S. Liu, D. Brunel, K. Sun, Y. Xu, F. Morlet-Savary, B. Graff, P. Xiao, F. Dumur, J. Lalevée, A monocomponent bifunctional benzophenone–carbazole type II photoinitiator for LED photoinitiating systems, Polym. Chem. 11 (2020) 3551–3556. https://doi.org/10.1039/D0PY00644K.
[36] C.Y. Barlow, D.C. Morgan, Polymer film packaging for food: An environmental assessment, Resources, Conservation and Recycling. 78 (2013) 74–80. https://doi.org/10.1016/j.resconrec.2013.07.003.
[37] J.L. Aparicio, M. Elizalde, Migration of Photoinitiators in Food Packaging: A Review, Packaging Technology and Science. 28 (2015) 181–203. https://doi.org/10.1002/pts.2099.
[38] M.A. Lago, A.R.-B. de Quirós, R. Sendón, J. Bustos, M.T. Nieto, P. Paseiro, Photoinitiators: a food safety review, Food Additives & Contaminants: Part A. 32 (2015) 779–798. https://doi.org/10.1080/19440049.2015.1014866.
[39] A.K. Nguyen, R.J. Narayan, Two-photon polymerization for biological applications, Materials Today. 20 (2017) 314–322. https://doi.org/10.1016/j.mattod.2017.06.004.
[40] G. Ye, H. Zhou, J. Yang, Z. Zeng, Y. Chen, Synthesis and characterization of oligomers containing the α-aminoalkylphenone chromophore as oligomeric photoinitiator, Journal of Applied Polymer Science. 99 (2006) 3417–3424. https://doi.org/10.1002/app.22956.
[41] E. Ay, Z. Raad, O. Dautel, F. Dumur, G. Wantz, D. Gigmes, J.-P. Fouassier, J. Lalevée, Oligomeric Photocatalysts in Photoredox Catalysis: Toward High Performance and Low Migration Polymerization Photoinitiating Systems., Macromolecules. 49 (2016) 2124–2134. https://doi.org/10.1021/acs.macromol.5b02760.
[42] P. Xiao, F. Dumur, M. Frigoli, M.-A. Tehfe, B. Graff, J.P. Fouassier, D. Gigmes, J. Lalevée, Naphthalimide based methacrylated photoinitiators in radical and cationic photopolymerization under visible light, Polym. Chem. 4 (2013) 5440–5448. https://doi.org/10.1039/C3PY00766A.
[43] J. Yang, W. Liao, Y. Xiong, Q. Wu, X. Wang, Z. Li, H. Tang, Naphthalimide dyes: Polymerizable one-component visible light initiators, Dyes and Pigments. 148 (2018) 16–24. https://doi.org/10.1016/j.dyepig.2017.08.053.
[44] J. Yang, C. Xu, Y. Xiong, X. Wang, Y. Xie, Z. Li, H. Tang, A Green and Highly Efficient Naphthalimide Visible Photoinitiator with an Ability Initiating Free Radical Polymerization under

Air, Macromolecular Chemistry and Physics. 219 (2018) 1800256. https://doi.org/10.1002/macp.201800256.
[45] J. Yang, W. Liao, Y. Xiong, X. Wang, Z. Li, H. Tang, A multifunctionalized macromolecular silicone-naphthalimide visible photoinitiator for free radical polymerization, Progress in Organic Coatings. 115 (2018) 151–158. https://doi.org/10.1016/j.porgcoat.2017.11.010.
[46] H. Chen, G. Noirbent, K. Sun, D. Brunel, D. Gigmes, F. Morlet-Savary, Y. Zhang, S. Liu, P. Xiao, F. Dumur, J. Lalevée, Photoinitiators derived from natural product scaffolds: monochalcones in three-component photoinitiating systems and their applications in 3D printing, Polym. Chem. 11 (2020) 4647–4659. https://doi.org/10.1039/D0PY00568A.
[47] H. Chen, G. Noirbent, Y. Zhang, K. Sun, S. Liu, D. Brunel, D. Gigmes, B. Graff, F. Morlet-Savary, P. Xiao, F. Dumur, J. Lalevée, Photopolymerization and 3D/4D applications using newly developed dyes: Search around the natural chalcone scaffold in photoinitiating systems, Dyes and Pigments. 188 (2021) 109213. https://doi.org/10.1016/j.dyepig.2021.109213.
[48] H. Chen, G. Noirbent, Y. Zhang, D. Brunel, D. Gigmes, F. Morlet-Savary, B. Graff, P. Xiao, F. Dumur, J. Lalevée, Novel D–π-A and A–π-D–π-A three-component photoinitiating systems based on carbazole/triphenylamino based chalcones and application in 3D and 4D printing, Polym. Chem. 11 (2020) 6512–6528. https://doi.org/10.1039/D0PY01197E.
[49] M.-A. Tehfe, F. Dumur, E. Contal, B. Graff, D. Gigmes, J.-P. Fouassier, J. Lalevée, Novel Highly Efficient Organophotocatalysts: Truxene–Acridine-1,8-diones as Photoinitiators of Polymerization, Macromolecular Chemistry and Physics. 214 (2013) 2189–2201. https://doi.org/10.1002/macp.201300362.
[50] M.-A. Tehfe, F. Dumur, B. Graff, J.-L. Clément, D. Gigmes, F. Morlet-Savary, J.-P. Fouassier, J. Lalevée, New Cleavable Photoinitiator Architecture with Huge Molar Extinction Coefficients for Polymerization in the 340–450 nm Range., Macromolecules. 46 (2013) 736–746. https://doi.org/10.1021/ma3024359.
[51] M.-A. Tehfe, J. Lalevée, S. Telitel, E. Contal, F. Dumur, D. Gigmes, D. Bertin, M. Nechab, B. Graff, F. Morlet-Savary, J.-P. Fouassier, Polyaromatic Structures as Organo-Photoinitiator Catalysts for Efficient Visible Light Induced Dual Radical/Cationic Photopolymerization and Interpenetrated Polymer Networks Synthesis, Macromolecules. 45 (2012) 4454–4460. https://doi.org/10.1021/ma300760c.
[52] N.A. Kazin, N.S. Demina, R.A. Irgashev, E.F. Zhilina, G.L. Rusinov, Modifications of 5,12-dihydroindolo[3,2-a]carbazole scaffold via its regioselective C2,9-formylation and C2,9-acetylation, Tetrahedron. 75 (2019) 4686–4696. https://doi.org/10.1016/j.tet.2019.07.015.
[53] M.-A. Tehfe, F. Dumur, B. Graff, F. Morlet-Savary, D. Gigmes, J.-P. Fouassier, J. Lalevée, Push–pull (thio)barbituric acid derivatives in dye photosensitized radical and cationic polymerization reactions under 457/473 nm laser beams or blue LEDs, Polym. Chem. 4 (2013) 3866–3875. https://doi.org/10.1039/C3PY00372H.
[54] P. Xiao, F. Dumur, B. Graff, F. Morlet-Savary, L. Vidal, D. Gigmes, J.P. Fouassier, J. Lalevée, Structural Effects in the Indanedione Skeleton for the Design of Low Intensity 300–500 nm Light Sensitive Initiators., Macromolecules. 47 (2014) 26–34. https://doi.org/10.1021/ma402149g.
[55] A. Bonardi, F. Bonardi, G. Noirbent, F. Dumur, C. Dietlin, D. Gigmes, J.-P. Fouassier, J. Lalevée, Different NIR dye scaffolds for polymerization reactions under NIR light, Polym. Chem. 10 (2019) 6505–6514. https://doi.org/10.1039/C9PY01447K.
[56] V. Nair, V. Nandialath, K.G. Abhilash, E. Suresh, An efficient synthesis of indolo[3,2-a]carbazoles via the novel acid catalyzed reaction of indoles and diaryl-1,2-diones, Org. Biomol. Chem. 6 (2008) 1738–1742. https://doi.org/10.1039/B803009J.
[57] A. Rieche, H. Gross, E. Höft, Über α-Halogenäther, IV. Synthesen aromatischer Aldehyde mit Dichlormethyl-alkyläthern, Chemische Berichte. 93 (1960) 88–94. https://doi.org/10.1002/cber.19600930115.
[58] I. Ramos-Tomillero, M. Paradís-Bas, I. De Pinho Ribeiro Moreira, J.M. Bofill, E. Nicolás, F. Albericio, Formylation of Electron-Rich Aromatic Rings Mediated by Dichloromethyl Methyl

Ether and TiCl4: Scope and Limitations, Molecules. 20 (2015) 5409–5422. https://doi.org/10.3390/molecules20045409.